On the Use of Battery-Electric Locomotive As A Grid-Support Service in Electric Power Systems

Farid Kochakkashani, Student Member, IEEE, Payman Dehghanian, Senior Member, IEEE, and Miguel A. Lejeune

Abstract—Harvesting wind energy is constrained by its generation availability and variability. Energy storage systems (ESSs) partly address this limitation by absorbing the generation volatility and curtailment. However, the conventional static ESSs may lack the necessary reach and versatility to effectively support large-scale power systems. This paper presents an innovative approach suggesting the use of battery-electric locomotives (BELs) as mobile energy reserve tools. The BEL carries separable battery railcars with enhanced storage capacity that offers a flexible and far-reaching energy supply. We propose a new uncertainty-aware optimization model that holistically integrates the operation of power and railway systems. The proposed model is formulated as a mixed-integer nonlinear stochastic programming (SMINLP) problem that incorporates uncertainty through joint probabilistic constraints (JPCs). Equivalent and tractable deterministic mixed-integer linear programming (MILP) reformulations are derived using the Boolean programming and the scenario-based approaches. The numerical tests showcase the superior scalability and computational efficiency of the Boolean method, especially when many scenarios are involved. The model is validated on the IEEE 6-bus test system and scaled up to the IEEE 118-bus test system, where comparative analyses reveal the model's ability to deliver cost-saving and congestion relief, with a particular emphasis on the responsiveness of separable battery railcars.

Index Terms—mobile power source; battery-electric locomotive (BEL); routing and scheduling; security-constrained unit commitment; joint probabilistic constraints; uncertainty.

NOMENCLATURE

A. Sets	
\mathcal{I},\mathcal{J}	Set of buses.
$\mathcal{G}\subset\mathcal{I}$	Set of generating units.
$\mathcal{I}^w \subset \mathcal{I}$	Set of buses connected to a wind farm.
$\mathcal A$	Set of arcs in the time-space network (TSN).
\mathcal{K}	Set of battery-electric locomotives (BEL).
\mathcal{W}	Set of battery railcars.
${\cal L}$	Set of transmission lines.
${\mathcal T}$	Set of hours.
${\mathcal S}$	Set of transportation time intervals.
$egin{aligned} \mathcal{A}_i^+ \ \mathcal{A}_j^- \end{aligned}$	Set of arcs in a TSN starting from station i .
\mathcal{A}_{i}^{-}	Set of arcs in a TSN ending at station j .
$\mathcal{H}^{'}$	Set of buses coupled with a railway station.
R Parameters	s and Constants

В.

Parameters	and Constants
a_u, b_u, r_u	Cost coefficients for generating unit u .
α_u, β_u	Start-up and shut-down costs of generating unit
	u.
$d_{k,(i,j)}$	Transportation cost of BEL k in arc (i, j) .
$\psi_{k,.}, \tilde{\psi}_{k,.}$	Initial and terminal state of BEL k at a station.
p_k^{max}	Maximum power exchange rate of BEL k .

F. Kochakkashani and P. Dehghanian are with the Department of Electrical and Computer Engineering, The George Washington University, Washington, DC 20052, USA (e-mails: kashani_farid@gwu.edu; payman@gwu.edu).

M. A. Lejeune is with the Department of Decision Sciences, The George Washington University, Washington, DC 20052, USA (e-mail: mlejeune@gwu.edu).

e_k^{\max}, e_k^{\min}	Maximum and minimum energy capacity of
	BEL k .
e_k^{te}	Terminal energy level in BEL k .
g_u^{max}, g_u^{min}	Maximum and minimum generation capacity
	of generating unit u .
$\overline{ ho}_u, \underline{ ho}_u$	Ramp-up and ramp-down rate limits of gener-
	ating unit u .
$f_l^{\rm max}$	Maximum capacity of transmission line l .
$arphi_t$	Spinning reserve requirement at time t .
$ au_u, ilde{ au}_u$	Minimum ON and OFF time requirements of
	generating unit u .
η	Predefined global reliability level.
ϱ_l	Reactance of transmission line l .
$\mu_{k,w}$	Energy capacity of battery railcar w in BEL k .

Power exchange efficiency in BEL k.

Power generation at bus i at time t.

C. Decision Variables

 γ_k

 $P_{i,t}$

0,0	\mathcal{C}
$P_{i,t}^w$	Wind power generation at bus i at time t .
$\Gamma_{u,t}$	Binary variable indicating the commitment sta-
	tus of generating unit u at time t .
$Y_{u,t}, Z_{u,t}$	Binary variables indicating startup and shut-
	down status of generating unit u at time t .
$R_{k,(i,j),s}$	Binary variable indicating travel status of BEL
	k on arc (i, j) at time interval s .
$P'_{k,i,t}$	Injected power of BEL k at bus i at time t .
$\begin{array}{c} P'_{k,i,t} \\ E_{k,t} \end{array}$	Energy stored in BEL k at time t .
$F_{l,t}$	Power flow on transmission line l at time t .
$\Theta^{'}_{t}$	Bus voltage angle difference at time t .

D. Random Variables

$\mathbf{p_{i,t}^d}$	Load demand at bus i at time t .
$\mathbf{p_{i,t}^w}$	Wind power at bus i at time t .
$\kappa_{i,s}$	Available capacity at classification yard i at
,	time interval s.

I. INTRODUCTION

THE significance of renewable power generation in electricity supply-demand balance cannot be overstated particularly considering the national push for electrification, decarbonization, and climate change mitigation [1]. The integration of renewable energy sources into power grids has the potential to lower power generation costs during periods of high demand. However, the accessibility to and variability of renewable energy generation pose significant challenges [2]. Nonetheless, advancements in energy storage system (ESS) technologies can effectively address spillage and fluctuations in energy production and enhance overall accessibility, thereby balancing electricity supply and demand. ESSs are designed and used either as stationary or mobile sources of power. Both stationary and mobile ESSs are promising sources for establishing a reliable and sustainable energy supply, each

offering distinct advantages and limitations. Stationary ESSs, such as large-scale battery systems and pumped hydro storage, are typically designed to store and distribute energy over a long period. On the other hand, mobile ESSs, such as portable batteries and fuel cells, can be transported and used locally to provide temporary or emergency power when needed.

A. Motivation and Background

The transportability of ESSs introduces an opportunity for spatiotemporal flexibility exchange; during nighttime hours, when electricity demand is typically low, wind speeds tend to be higher, leading to increased power generation potential from wind turbines. However, wind curtailment (spillage) may occur since the electricity grid cannot fully absorb this excess energy during the low-demand night hours. In such cases, an opportunity arises to capture the curtailed energy and utilize it for battery charging. With this excess energy stored in batteries during periods of low demand, it can be later discharged and supplied back to the grid during daytime peak demand periods, thus maximizing the utilization of renewable energy [3]. Mobile ESSs provide greater flexibility as they can be transported across time and space to meet energy demands. They also offer a more cost-effective solution for energy supply in remote or inaccessible areas [4], as they do not require the installation of complex and often costly infrastructure. In addition, mobile ESSs can be employed in emergency scenarios to provide power to critical facilities and support disaster relief efforts [5]-[7]. An overview of the stateof-the-art mobile power source technologies, sizes, capacities, and costs is provided in [8], [9].

Acting as mobile ESSs, BELs serve as promising means of transporting batteries; BELs can accommodate multiple containers of batteries, enabling the transportation of substantial amounts of energy over extended distances. This makes BELs a desirable strategy for energy transportation and distribution through the railway system. Further, BELs offer advantages such as the ability to transport batteries disregarding road infrastructure or drivers' incentives. In order to leverage the advantages offered by BELs, it is important to recognize the inherent uncertainty [10] associated with renewable energy generation, demand patterns, and transportation. Embracing a risk-averse approach becomes essential to ensure the reliability of the power system [11], safeguard it against potential disruptions, and optimize the utilization of mobile ESS capabilities.

B. Literature Survey

The concept of transporting mobile energy storage through railways is first put forward by [12], where battery-based energy storage transportation (BEST) is introduced. With the goal of evaluating its contribution to the power grid operation, particularly in the security-constrained unit commitment (SCUC) problem, a mixed-integer linear programming (MILP) model is developed. The model takes into account the train routing and dispatch decisions. The contribution of such a technology is shown to be reflected in the system operation cost and line congestion reduction. Addressing the model scalability and computational complexities, [13] further complements [12] by using the Lagrangian decomposition method to solve the large-scale problem faster. Reference [14]

builds on top of the previous models by incorporating into the model uncertainties in load, renewable generation forecast, and failures in power and transportation networks. Further addressing the mobile energy storage problem in railway systems, reference [15] proposes a multi-objective stochastic programming model to minimize the system operation cost and greenhouse gas emissions taking into account the uncertainties in renewable generation and load. Reference [16] develops a robust optimization model for techno-economic assessment of mobile battery ESSs in day-ahead scheduling of an integrated power and railway network. Reference [17] introduces a twostage robust-stochastic model to analyze the BEST system in a day-ahead market-clearing problem using information-gap theory. Reference [18] provides a multi-objective two-stage stochastic program for the railway-based storage system in a unit commitment model, where 7% and 20% reductions in system operation cost and carbon emissions, respectively, are achieved. In [19], BESTs and stationary ESSs are used in a transmission planning problem with a focus on line congestions. Reference [20] proposes a multi-stage optimization model to address the transportation and logistics of railwaybased batteries charged with renewable energy. Unlike the previous studies focusing on system operation, this study investigates the role of mobile ESSs from the transportation system perspective and applies train transportation and carpooling strategies. A similar study in [21] develops a twostage optimization model that considers battery transportation and evaluates its contribution to peak load shaving.

With the goal to transport battery storage systems through railways, BEL scheduling and dispatch become critical decisions to make, the research on which is under-explored in the literature. Reference [22] proposes a stochastic programming model for single-track train dispatching, where schedules are optimized periodically over a rolling horizon while robust meet-pass plans are selected and disseminated for each roll period. Reference [23] develops a bi-objective stochastic program to model a railway traffic scheduling problem where optimal train sequencing and routing decisions are made in conjunction with short-term maintenance plans. Reference [24] delineates an MILP model to investigate the effect of disruptions or congestion in railway transportation systems on train routing decisions. In [25], railway transportation scheduling and maintenance are integrated into an MILP formulation. In [26], a multi-objective optimization model is proposed to minimize passenger travel time and maintenance costs. In order to optimize a train rescheduling problem with track emergency maintenance, [27] introduces a mixed-integer nonlinear programming model that reduces the system delay and alleviates the track disruptions.

In the context of integrated railway and power networks, a dominant conservative assumption in the literature is that BELs, which are required to get charged or discharged, spend an entire time span in a given station for power exchange. Additionally, the existing literature did not consider the separability of the railcars for spatiotemporal energy delivery. The existing models are also reported to be computationally complex particularly under real-world conditions where prevailing uncertainties in both power and railway systems are present.

C. Problem Statement and Proposed Contributions

We study the daily operation of the power system through the SCUC problem, where BEL is integrated as a large-scale mobile ESS for power delivery across the power transmission system. This allows for a spatiotemporal dispatch of batteries during the day across a larger geographical region and features maximum wind utilization. To the best of our knowledge, this paper establishes a pioneering approach that introduces probabilistic constraints to address the complex integration of day-to-day power system operations with the transportation of mobile power sources via railways. We design a riskaverse approach promoting reliability through the incorporation of probabilistic constraints. In contrast to the existing power system models with individual chance constraints (see review paper [28]), the proposed model incorporates a joint probabilistic constraint (JPC) that establishes a networkwide reliability level. An equivalent reformulation approach is introduced to convert the stochastic mixed-integer nonlinear nonconvex problem into a deterministic MILP.

The core contributions of this paper are listed as follows.

- A novel stochastic optimization model with JPCs is proposed for the integration of BEL in power system operation that effectively captures the uncertainty in wind generation, demand, and classification yards capacity.
- The proposed model captures the railway system's critical characteristics, including traffic, collision avoidance, and the limited capacity of the classification yards. Also, the battery railcars carried by the BELs are considered *separable* as the BELs can detach battery railcars in any classification yard and the remaining railcars can then be dispatched to the next destination. The separability feature enables the transportation system to be more responsive and deliver the required power faster.
- The intricacy of the JPCs is addressed through a stateof-the-art Boolean reformulation method with a computationally efficient formulation that is solved quickly even when many scenarios are considered. This in turn enables capturing a vast array of uncertainty features and gives a more dependable problem representation.

The remainder of the paper is organized as follows. Section II provides the problem formulation and section III presents the reformulation method. Numerical case studies on the IEEE 6-bus and 118-bus test systems are conducted in Section IV. Section V offers perspectives on framework applicability and the conclusions are provided in Section VI.

II. PROBLEM FORMULATION

This section introduces a stochastic mixed-integer nonlinear optimization model with JPCs (referred to as **SMINLP-JPC**) that accounts for the integration of mobile power sources through railways into the SCUC problem. The quadratic cost objective function includes two components and reads:

 \min

$$\sum_{t \in \mathcal{T}} \sum_{u \in \mathcal{G}} \left[\left(a_u P_{u,t}^2 + b_u P_{u,t} + r_u \Gamma_{u,t} \right) + \alpha_u Y_{u,t} + \beta_u Z_{u,t} \right]$$

$$+ \sum_{k \in \mathcal{K}} \sum_{s \in \mathcal{S}} \sum_{(i,j) \in \mathcal{A}} d_{k,(i,j)} R_{k,(i,j),s}$$

$$\tag{1}$$

The objective function (1) minimizes the sum of the power generation costs from thermal generating units and the transportation costs. The first term represents the power generation and the unit startup and shutdown costs while the second one is related to the railway transportation costs. The optimization model considers multiple constraints associated with various components, including the TSN, BELs, batteries, power system operation, generating units, and transmission lines.

A. BEL Constraints in TSN

Constraints (2a) and (2b) set the initial and terminal status of the BELs in the TSN. Constraints (2c) indicate that each BEL must be at one arc at each time span s. The collision avoidance constraints (2d) assert that BELs cannot traverse both arcs (i,j) and (j,i) at the same time and define the arc capacity, allowing for at most one BEL per arc. The JPCs (2e) ensure that the number of trains at each station with a classification yard does not exceed the capacity of the yard with a predetermined probability. Unlike individual probabilistic constraints, the JPC formulation ensures systemwide reliability across all transportation nodes. Constraints (2f) establish the arrival and departure balance for the BELs. That is, if BEL k reaches station i at time t, the next station visited by BEL k at time t+1 must be a station connected to station i. At the end of the operating horizon, the detached battery railcars are gathered through an empty freight car schedule to get recharged overnight for the next-day dispatch.

$$\sum_{(i,j)\in\mathcal{A}_i^+} R_{k,(i,j),1} = \psi_{k,i}, \qquad k \in \mathcal{K}, i \in \mathcal{I}$$
 (2a)

$$\sum_{(i,j)\in\mathcal{A}_{j}^{-}}R_{k,(i,j),|S|}=\tilde{\psi}_{k,j}, \qquad k\in\mathcal{K}, i\in\mathcal{I} \quad (2b)$$

$$\sum_{(i,j)\in\mathcal{A}} R_{k,(i,j),s} = 1, \qquad s \in \mathcal{S}, k \in \mathcal{K}$$
 (2c)

$$\sum_{k \in \mathcal{K}} (R_{k,(i,j),s} + R_{k,(j,i),s}) \le 1,$$
(2d)

$$(i,j) \in \mathcal{A} : i \neq j, s \in \mathcal{S} \setminus \{|S|\}$$

$$\mathbb{P} \left(\sum_{k \in \mathcal{K}} R_{k,(i,j),s} \leq \kappa_{i,s}, \ (i,j) \in \mathcal{A} : i = j \right) \geq \eta, \ s \in \mathcal{S}$$

$$\sum_{(i,j)\in\mathcal{A}_{i}^{+}} R_{k,(i,j),s+1} = \sum_{(i,j)\in\mathcal{A}_{i}^{-}} R_{k,(i,j),s},$$

$$s \in \mathcal{S} \setminus \{|\mathcal{S}|\}, k \in \mathcal{K}, i \in \mathcal{I}$$
(2e)

B. Battery Capacity and Discharging Constraints

The constraints (3a) govern the discharging of energy from BELs at transmission buses, while (3b) define the acceptable energy capacity range for each BEL. Constraints (3c) capture the energy balance of the BELs during discharge. Due to the separability of the battery railcars, the energy discharged from any BEL must be a multiplier of the railcar capacity. These constraints are nonconvex due to the roundup function. Constraints (3d) set the terminal value for the energy stored in BEL k at the last period.

$$0 \leq P'_{k,j,t} \leq R_{k,(i,j),s} \ p_k^{max}, \\ k \in \mathcal{K}, i,j \in \mathcal{H}, s \in \mathcal{S}, t \in \mathcal{T}$$
 (3a)
$$e_k^{min} \leq E_{k,t} \leq e_k^{max}, \qquad k \in \mathcal{K}, t \in \mathcal{T}$$
 (3b)
$$E_{k,t} = E_{k,t-1} - \sum_{j \in \mathcal{H}} \left\lceil \frac{P'_{k,j,t}}{\mu_{k,w}} \right\rceil \mu_{k,w}, \quad k \in \mathcal{K}, w \in \mathcal{W}, t \in \mathcal{T}$$
 (3c)

$$E_{k,|\mathcal{T}|} = e_k^{te},$$
 $k \in \mathcal{K}$ (3d)

C. Power System Constraints

The proposed JPC (4a) contains three sets of stochastic inequalities with random right-hand side vectors. These constraints establish the system's power balance for meeting the demand and impose limits for wind power generation based on its predicted generation level. The source of uncertainty is due to the imperfect prediction of load and wind energy generation. The JPC requires the many stochastic inequalities to hold jointly with probability at least equal to η . Constraints (4b) define the system spinning reserve limits and are nonconvex due to the bilinear terms involving the multiplication of a binary variable by a continuous one.

$$\mathbb{P}\begin{pmatrix} \sum_{(i,j)\in\mathcal{L}} F_{l,t} - \sum_{(j,i)\in\mathcal{L}} F_{l,t} - P_{i,t} - P_{i,t}$$

$$\sum_{u \in \mathcal{G}} \Gamma_{u,t} (g_u^{max} - P_{u,t}) + \sum_{k \in \mathcal{K}} \sum_{i \in \mathcal{H}} \sum_{j \in \mathcal{H}} R_{k,(i,j),s} (p_k^{max} - P'_{k,i,t}) \ge \varphi_t, \quad t \in \mathcal{T}$$

$$(4b)$$

D. Generating Unit Constraints

Each constraint (5a) specifies the capacity limit of the corresponding generating unit. The ramp-up and ramp-down limits of the generating units are enforced by (5b) and (5c). Constraints (5d) and (5e) define the minimum on and off time of the generating units. Constraints (5f) establish the linkage between the unit commitment and the startup or shutdown indicator variables. Each constraint (5g) enforces that the generating unit u cannot shut down and start up concomitantly.

$$\Gamma_{u,t} g_u^{min} \le P_{u,t} \le \Gamma_{u,t} g_u^{max}, \qquad u \in \mathcal{G}, t \in \mathcal{T}$$
 (5a)

$$P_{u,t} - P_{u,t-1} \le \overline{\rho}_u (1 - Y_{u,t}) + g_u^{min} Y_{u,t},$$

$$u \in \mathcal{G}, t \in \mathcal{T}$$
(5b)

$$P_{u,t-1} - P_{u,t} \le \underline{\rho}_u (1 - Z_{u,t}) + g_u^{min} Z_{u,t},$$

$$u \in \mathcal{G}, t \in \mathcal{T}$$
(5c)

$$Y_{u,t} \le \Gamma_{u,m}, \quad u \in \mathcal{G}, t \in \mathcal{T}, m \in [t, min(\tau_u + t, |\mathcal{T}|)]$$
 (5d)

$$Z_{u,t} \le 1 - \Gamma_{u,m},$$

$$u \in \mathcal{G}, t \in \mathcal{T}, m \in [t, \min(\tilde{\tau}_u + t, |\mathcal{T}|)]$$
(5e)

$$Y_{u,t} - Z_{u,t} \le \Gamma_{u,t} - \Gamma_{u,t-1},$$
 $u \in \mathcal{G}, t \in \mathcal{T}$ (5f)
 $Y_{u,t} + Z_{u,t} \le 1,$ $u \in \mathcal{G}, t \in \mathcal{T}$ (5g)

E. Transmission Line Constraints

Constraints (6a) and (6b) enforce the lower and upper bounds on the power flow based on the capacity of the transmission line. Note that transmission lines are often operated below their full potential capacity, typically at around 70% of their rated capacity, to ensure system reliability and avoid overloading. However, in the presence of reliable mobile power sources, there may be an opportunity to leverage this flexibility to increase the effective capacity of the transmission lines and enhance the overall system performance and reliability.

$$-f_{l}^{max} \leq F_{l,t} \leq f_{l}^{max}, \qquad \qquad l \in \mathcal{L}, t \in \mathcal{T} \quad \text{(6a)}$$

$$F_{l,t} = \frac{\Theta_{i,t} - \Theta_{j,t}}{\varrho_{l}}, \qquad \qquad l, (i,j) \in \mathcal{L}, t \in \mathcal{T} \quad \text{(6b)}$$
III. REFORMULATION METHOD

We first outline in Section III-A a set of reformulation techniques that provide a linear reformulation of the nonconvex terms in the deterministic constraints (3c) and (4b). Next, in Section III-B, we delve into the exact and deterministic reformulation of the JPCs (2e) and (4a).

A. Convexification of Nonlinear Deterministic Constraints

Constraint (4b) contains two types of bilinear terms which are both nonlinear and nonconvex. Additionally, (3c) involves the quasilinear roundup function, which is discontinuous and nondifferentiable. We first linearize the bilinear terms in (4b). We introduce the auxiliary variables $Q_{k,i,j,s,t}$, each set equal to $R_{k,i,j,s}P'_{k,i,t}$ via the McCormick inequalities [29]:

$$Q_{k,i,j,s,t} \le P'_{k,i,t}, \quad k \in \mathcal{K}, i \in \mathcal{I}, j \in \mathcal{J}, s \in \mathcal{S}, t \in \mathcal{T}$$
 (7a)

$$Q_{k,i,j,s,t} \le p_k^{max} \ R_{k,i,j,s},$$

$$k \in \mathcal{K}, i \in \mathcal{I}, j \in \mathcal{J}, s \in \mathcal{S}, t \in \mathcal{T}$$
(7b)

$$Q_{k,i,j,s,t} \ge P'_{k,i,t} - (1 - R_{k,i,j,s}) p_k^{max},$$

$$k \in \mathcal{K}, i \in \mathcal{I}, j \in \mathcal{J}, s \in \mathcal{S}, t \in \mathcal{T}$$
(7c)

$$Q_{k,i,j,s,t} \ge 0,$$
 $k \in \mathcal{K}, i \in \mathcal{I}, j \in \mathcal{J}, s \in \mathcal{S}, t \in \mathcal{T}$ (7d)

Similarly, the McCormick inequalities (8a)-(8d) linearize each bilinear term $P_{u,t}\Gamma_{u,t}$ in (4b) and set each auxiliary variable $D_{u,t}$ equal to $P_{u,t}\Gamma_{u,t}$:

$$min[0, g_u^{min}] \le D_{u,t} \le g_u^{max}, \qquad u \in \mathcal{G}, t \in \mathcal{T}$$
(8a)
$$g_u^{min}\Gamma_{u,t} \le D_{u,t} \le g_u^{max}\Gamma_{u,t}, \qquad u \in \mathcal{G}, t \in \mathcal{T}$$
(8b)

$$\begin{split} P_{u,t} - (1 - \Gamma_{u,t}) g_u^{max} &\leq D_{u,t} \leq \\ P_{u,t} - (1 - \Gamma_{u,t}) g_u^{min}, & u \in \mathcal{G}, t \in \mathcal{T} \\ D_{u,t} &\leq P_{u,t} + (1 - \Gamma_{u,t}) g_u^{max}, & u \in \mathcal{G}, t \in \mathcal{T} \end{split} \tag{8c}$$

Let ϵ be an infinitesimal positive number. To linearize the term in the roundup function in (3c), we follow the approach proposed in [30] and introduce an auxiliary integer-valued decision variable $\overline{P}_{k,i,t}$ (9b) and the following constraints

$$\frac{P'_{k,i,t}}{\mu_{k,w}} \le \overline{P}_{k,i,t} \le \frac{P'_{k,i,t}}{\mu_{k,w}} + 1 - \epsilon,$$

$$k \in \mathcal{K}, w \in \mathcal{W}, i \in \mathcal{I}, t \in \mathcal{T}$$

$$\overline{P}_{k,i,t} \in \mathbb{Z}, \qquad \qquad k \in \mathcal{K}, i \in \mathcal{I}, \ t \in \mathcal{T} \ \ (9b)$$
 which ensure $\overline{P}_{k,i,t} = \left\lceil \frac{P'_{k,i,t}}{\mu_{k,w}} \right\rceil, k \in \mathcal{K}, w \in \mathcal{W}, i \in \mathcal{I}, t \in \mathcal{T}.$ The above techniques applied to (3c) and (4b) give us a mixed-integer linear reformulation of the deterministic constraints.

B. Deterministic Reformulation of JPCs

In order to reformulate the JPCs (2e) and (4a), two reformulation techniques, i.e., the scenario-based and the Boolean modeling approaches [31], are utilized. To present them, we introduce a generic form of a JPC

$$\mathbb{P}(h_m X \ge \boldsymbol{\xi_m}, \ m \in \mathcal{M}) \ge p \ , \tag{10}$$

with an \mathcal{M} -dimensional random right-hand side vector $\boldsymbol{\xi}$ and reliability level p. The notation h represents a vector of fixed parameters. The random vector $\boldsymbol{\xi}$ follows a joint $|\mathcal{M}|$ -variate probability distribution with finite support. The set of possible realizations is defined as Ω . Each realization $k \in \Omega$ is represented by an $|\mathcal{M}|$ -dimensional deterministic vector $\omega^k = [\omega_1^k, \ldots, \omega_M^k]$ and defines a value that the random vector can take with probability p^k , such that $\sum_{k \in \Omega} p^k = 1$. The notation $F(\omega^k) = \mathbb{P}(\boldsymbol{\xi} \leq \omega^k)$ defines the cumulative distribution function of the random vector while its marginal probability distributions are $F_m(w_m^k) = \mathbb{P}(\boldsymbol{\xi}_m \leq \omega_m^k), m \in \mathcal{M}$.

The **scenario-based reformulation** associates a binary variable λ^k to each realization, and each constraint (11a) verifies if the conditions imposed by the associated realization are satisfied. If not, the corresponding decision variable λ_k is forced to take value 1. The joint reliability level is achieved by upper-bounding to (1-p) the sum of the probabilities of the unsatisfied realizations (11b). The scenario-based reformulation of JPC (10) is given next:

$$h_m X \ge \omega_m^k (1 - \lambda^k),$$
 $m \in \mathcal{M}, k \in \Omega$ (11a)

$$\sum_{k \in \Omega} p^k \lambda^k \le 1 - p \tag{11b}$$

$$\lambda \in \{0, 1\}^k \tag{11c}$$

Using the scenario approach, we obtain the following reformulation for problem **SMINLP-JPC**:

MILP-SR: $\min(1)$

s.to
$$(2a) - (2d); (2f) - (3d); (4b) - (9b)$$

 $-\sum_{k' \in \mathcal{K}} R_{k',(i,j),s} \ge \omega_{i,s}^k (1 - \lambda_s^k),$
 $k \in \Omega, (i,j) \in \mathcal{A} : i = j, s \in \mathcal{S}$ (12a)

$$\sum p_s^k \lambda_s^k \le 1 - p \qquad \qquad s \in \mathcal{S} \tag{12b}$$

$$\sum_{(i,j)\in\mathcal{L}} F_{l,t} - \sum_{(j,i)\in\mathcal{L}} F_{l,t} - P_{i,t} - P_{i,t}^w - \sum_{k'\in\mathcal{K}} \gamma_{k'} P'_{k',i,t}$$
(12c)

$$\geq \omega_{i,t}^{k}(1 - \Lambda_{t}^{k}), \qquad k \in \Omega, i \in \mathcal{I}, t \in \mathcal{T}$$
$$-P_{i,t}^{w} \geq \bar{\omega}_{i,t}^{k}(1 - \Lambda_{t}^{k}), \qquad k \in \Omega, i \in \mathcal{I}^{w}, t \in \mathcal{T}$$
(12d)

$$\sum_{k \in \Omega} p_t^k \Lambda_t^k \le 1 - p \qquad \qquad t \in \mathcal{T} \tag{12e}$$

$$\lambda, \Lambda \in \{0, 1\}^k \tag{12f}$$

The linear inequalities (12a)-(12b) and (12c)-(12f) reformulate the JPCs (2e) and (4a), respectively. Needless to say, the tractability of the reformulation is directly related to the number of scenarios as one binary variable and one constraint are added for each scenario.

We now reformulate the JPCs with the Boolean programming method which entails two major steps outlined

in pseudo-code 1 and provides a mixed-integer linear reformulation of the feasible set defined by the JPCs.

We first introduce the p-sufficiency concept [31] which plays a pivotal role. A realization ω^k is p-sufficient if $F(\omega^k) \geq p$ and is p-insufficient otherwise. Any p-sufficient realization defines sufficient conditions for (10) to hold. Necessary conditions to qualify as p-sufficient can be derived from the so-called univariate-quantile inequalities, which require ω^k to satisfy: $F_m(\omega_m^k) \geq p, m = 1, \ldots, |\mathcal{M}|$.

The next step is the construction of the set of recombinations $\overline{\Omega}$ [32] defined as $\overline{\Omega} = C_1 \times C_2 \times \ldots \times C_{|\mathcal{M}|}$ [31] with

$$C_m=\{\omega_m^k: F_m(\omega_m^k)\geq p, k\in\Omega\}, m\in\mathcal{M}$$
 (13) representing the sets of values that ξ_m can take and that are larger than the p -quantile of F_m . The set of recombinations includes all vectors ω^k that satisfy the univariate-quantile inequalities and can possibly be p -sufficient. The elements of each set $C_m, m\in\mathcal{M}$, called cut points [31], are thereafter denoted by $\{c_{m,1},\ldots,c_{m,\nu_m}\}\in C_m$, where ν_m is the number of cut points for each random variable ξ_m . Without loss of generality, we arrange the cut points in ascending order: $c_{m,1}< c_{m,2}<\ldots< c_{m,\nu_m}$. The recombination set is then split into two collectively exhaustive and disjoint subsets $\overline{\Omega}^+:=\{\omega^k\in\overline{\Omega}:F(\omega^k)\geq p\}$ and $\overline{\Omega}^-:=\{\omega^k\in\overline{\Omega}:F(\omega^k)< p\}$, respectively, denoting the sets of p -sufficient and p -insufficient recombinations.

The next step is to binarize [31] the probability distribution and the recombinations. The binarization process uses the cut points to map each numerical recombination vector ω_m^k to a binary vector of $\beta_m^k = [\beta_{m,1}^k, \ldots, \beta_{m,\nu_m}^k]$ and proceeds as follows: $\beta_{m,o}^k = 1$ if $\omega_m^k \geq c_{m,o}$ and $\beta_{m,o}^k = 0$ otherwise for all $m \in \mathcal{M}, o = 1, \ldots, \nu_m$. This means that the o^{th} binary attribute $\beta_{m,o}^k$ corresponding to random variable ξ_m in realization k takes value 1 if the value of ω_m^k is larger than or equal to the cut point $c_{m,o}$. Since we have $c_{m,o} < c_{m,o+1}, o < \nu_m - 1$, it follows from the binarization that: $\beta_{m,o}^k \geq \beta_{m,o+1}^k, k \in \bar{\Omega}, m \in \mathcal{M}, 1 \leq o < \nu_m - 1$.

As shown in [32] and [33], the binarization process allows for the derivation of a partially defined Boolean function (pdBf) whose truth table represents exactly the feasible area of the JPC (10) as long as the set of cut points used for the binarization process is consistent. The sufficient-equivalent set of cut points (13) fulfills this condition (see [31]); it is injective over $\overline{\Omega}$, which guarantees that the sets Ω_B^+ and Ω_B^- of p-sufficient and p-insufficient binarized recombinations are disjoint: $\Omega_B^+ \cap \Omega_B^- = \emptyset$. Using the properties of threshold Boolean functions (see [32]), the following constraints can be extracted from the pdBf representing the feasible area of (10) to represent it with mixed-integer linear inequalities:

$$\sum_{m \in \mathcal{M}} \sum_{n=1}^{\nu_m} \beta_{m,n}^k U_{m,n} \le |\mathcal{M}| - 1, \qquad k \in \Omega_B^-$$
 (14a)

$$\sum_{m=1}^{\nu_m} U_{m,n} = 1, \qquad m \in \mathcal{M}$$
 (14b)

$$h_m X \ge \sum_{n=1}^{\nu_m} c_{m,n} U_{m,n}, \qquad m \in \mathcal{M} \quad (14c)$$

$$U \in \{0, 1\}^{m \times n} \tag{14d}$$

The set of knapsack constraints (14a) ensures that no p-insufficient realization in Ω_B^- is covered [32]. In other words, the recombination defined by the binary vector U (14d) is not p-insufficient, and is by corollary p-sufficient. The partitioning constraints (14b) require that exactly one of the ν_m binary variables $U_{m,n}$ (14d) associated with the admissible values for each $\xi_{\mathbf{m}}, \mathbf{m} \in \mathcal{M}$ must be equal to 1. The juxtaposition of (14a) and (14b) implies that the vector $\left[\sum_{n=1}^{\nu_1} c_{1,n} U_{1,n}, \ldots, \sum_{n=1}^{\nu_{|\mathcal{M}|}} c_{|\mathcal{M}|,n} U_{|\mathcal{M}|,n}\right]$ corresponds to a p-sufficient recombination. Therefore, constraint (14c) requires the satisfaction of all the conditions defined by a p-sufficient recombination, which ensures that the JPC (10) holds true.

Using the above-described Boolean reformulation method, we obtain the following MILP reformulation equivalent to problem **SMILP-JPC**:

MILP-BR: min (1)

$$s.to$$
 (2a) - (2d); (2f) - (3d); (4b) - (9b)

$$-\sum_{k \in \mathcal{K}} R_{k,(i,j),s} \ge \sum_{n=1}^{\nu_i} c_{i,n,s} U_{i,n,s},$$
(15a)
$$(i,j) \in \mathcal{A} : i = j, s \in \mathcal{S}$$

$$\sum_{i \in \mathcal{H}} \sum_{n=1}^{\nu_i} \beta_{i,n,s}^{1,k} U_{i,n,s} \le |\mathcal{I}| - 1, \qquad s \in \mathcal{S}, k \in \Omega_B^- \text{ (15b)}$$

$$\sum_{i=1}^{\nu_i} U_{i,n,s} = 1, \qquad i \in \mathcal{RS}, s \in \mathcal{S} \text{ (15c)}$$

$$\sum_{n=1}^{\nu_i} F_{l,t} - \sum_{(j,i) \in L} F_{l,t} - P_{i,t} - P_{i,t}^w - P_{i,t}^w - P_{i,t}^w - P_{i,t}^w = P_{i,t}^w \ge \sum_{n=1}^{\nu_i} c'_{i,n,t} U'_{i,n,t}, \qquad i \in \mathcal{I}, t \in \mathcal{T}$$

$$-P_{i,t}^w \ge \sum_{n=1}^{\bar{\nu}_i} \bar{c}_{i,n,t} \bar{U}_{i,n,t}, \qquad i \in \mathcal{I}, t \in \mathcal{T} \text{ (15e)}$$

$$\sum_{i \in \mathcal{I}} \sum_{n=1}^{\nu_i} \beta_{i,n,t}^{2,k'} U'_{i,n,t} + \sum_{i \in \mathcal{I}^w} \sum_{n=1}^{\bar{\nu}_i} \beta_{i,n,t}^{3,k'} \bar{U}_{i,n,t} \le P_{i,t}^w - P_{i,t}^w = P_{i,t}^w - P_{i,t}^w = P_{i,t}^w - P_{i,t}^w = P_{i,t}^w - P_{i,t}^w = P_{i,t}^w - P_{i,t}^w -$$

Inequalities (15a)-(15c) and (15d)-(15i) reformulate the JPC (2e) and (4a), respectively, into deterministic forms.

IV. NUMERICAL RESULTS

We now evaluate the performance of the proposed model for the rail-based ESS integrated into the daily operation of the power system on two test systems. The proposed methodology is first tested on an IEEE 6-bus test system [12] to simply illustrate the effectiveness of the designed framework. The IEEE 118-bus test system [14] is then used to demonstrate the scalability of the approach. The formulation considers DC

Algorithm 1: Boolean Reformulation Method

```
Data: \omega^k, F(\omega^k), F_m(\omega_m^k), JPC (10)
Result: C_m, \beta_{m,n}^k, \Omega_B, \Omega_B^+, \Omega_B^-, MILP Reformulation
 1 for \{k \in \Omega, m \in \mathcal{M}\} do
               if F_m(\omega_m^k) \geq p then
 3
                      C_m \leftarrow \omega_m^k;
 5 end
 6 \bar{\Omega} \leftarrow C_1 \times C_2 \times ... \times C_{|\mathcal{M}|}
 7 for k \in \overline{\Omega} do
               if F(\omega^k) \geq p then
                       \dot{\overline{\Omega}}^+ \leftarrow \omega^k;
             \bigcap_{i} \overline{\Omega}^- \leftarrow \omega^k; end
10
11
12
              \begin{array}{l} \text{if } \omega_m^k \geq c p_{m,n} \text{ then} \\ \mid \ \beta_{m,n}^k \leftarrow 1; \\ \text{else} \end{array}
13
14
15
16
17
     Binary projection : (\Omega_B, \Omega_B^+, \Omega_B^-) \leftarrow (\overline{\Omega}, \overline{\Omega}^+, \overline{\Omega}^-)
20 MILP reformulation of feasible set of (10) with (14c)-(14d)
```

power flow model, while details on the use of AC power flow formulation in the proposed framework are provided in the electronic Appendix [34]. A comparison between two exact reformulation methods is drawn based on runtime and model size – the number of constraints and binary variables –, all pivotal for model tractability. The stochastic models are evaluated across cases of 100, 1,000, 2,000, and 10,000 scenarios. Unless specified, the results in this section pertain to the 10,000-scenario instance. The optimization models are solved on a PC with an Intel i7-7700 processor and 16GB memory. The problems are formulated using AMPL and solved with the optimization solver Gurobi 10.0.0.

The data are collected from the existing literature [12]-[18]. The 6-bus system is assumed to be connected to a railway network consisting of three railway stations, while the 118-bus test system is connected to an eight-station railway network. The transportation cost between each pair of nodes is considered to be \$50. Due to the separable design of the railcars, the BELs can detach the battery railcars quickly and stay on-call for any possible request on the power grid. The capacity of railway stations with classification yards is exogenous and depends on other trains or BELs in the yard. Moreover, collision avoidance and traffic considerations are incorporated into the TSN. Based on the capacity of battery railcars, each railcar can provide 20 MWh of energy or an equivalent amount of 10 MW power. As a result of recent technological advancements and the energy density of presently available batteries, lithium-ion batteries exhibit a high energy density of 250 watthour per kilogram (Wh/kg) [35]. It is reported in some recent studies that their energy density is as high as 300 watthour per kilogram (Wh/kg) [36]. Accordingly, the capacity of a standard railcar is 100 tons [37]. Hence, it can be determined that a train railcar could transport a battery with 30 MWh in capacity. Our assumption of 20 MWh batteries for each battery railcar proves to be tenable and in line with the evolving technology. The number of battery

TABLE I OPTIMAL BEL DISPATCH IN Case I: IEEE 6-Bus Test System

Time span	1	2	3	4	5	6	7	8	9	10	11	12	Total
Route (Station i -Station j)	1-4	4-4	4-4	4-4	4-4	4-4	4-4	4-4	4-4	4-4	4-4	4-1	Operation Cost:
Required battery railcars	0	0	1	1	0	0	0	2	0	2	0	0	\$95,326.75

railcars attached to BELs varies across the test cases.

Note that this work addresses the problem from its system operator perspective. The BEL scheduling is carried out with the oversight of railway dispatchers and regional control centers who are in charge of train scheduling and traffic management in the railway system [38]. An assumption is made that the power system operator already owns a railway infrastructure or can utilize the infrastructure of a third party (with a high priority) to schedule the BELs. Either way, the power system operator must come up with an initial optimal itinerary for the BELs before assessing next the feasibility of the schedule. The proposed model in this study provides the initial schedule for the power system operator. The system operator can replicate a customized study if their external factors are different from the ones assumed in this work. Such limitations can be expressed in the proposed model using linear constraints imposing bounds on the availability of the railroad arcs $(R_{k,(i,j),s})$.

A. Case I: IEEE 6-Bus Test System

The IEEE 6-bus test system consists of three generating units, seven transmission lines, and three load points, and is connected to a three-station railway system. One wind farm with a generation capacity of 30 MW is connected to the power grid at bus 1. The single BEL considered in this case consists of six battery railcars with a capacity amounting to 60MW power or 120 MWh energy, on aggregate. A holistic view of the integrated networks is shown in Fig. 1. The optimal operation cost with the SMINLP-JPC model amounts to \$95,326.75. The BEL route and the required number of battery railcars are shown in Table I. As evident from this table, the BEL travels to bus 4 and stays there until the end of the scheduling horizon when it travels back to the origin bus. The railway system does not force BELs to move all the time. In some cases, BELs can remain stationary and yet relieve the transmission line congestion. Furthermore, the optimization model generates the BEL schedule ahead of time. Hence, when detaching the battery railcars is not required, the railcars can stay attached to the BEL and get back to the origin at the end of the scheduling horizon. The value of the proposed framework is evident when comparing system performance with and without the incorporation of BELs. The presence of BELs results in a 5.2% saving in daily operational costs compared to their absence (\$100,553.58)-see Table I.

B. Case II: IEEE 118-Bus Test System

The IEEE 118-bus test system (see Fig. 3) is used to verify the scalability of the proposed model. This system includes 54 thermal generating units, 186 transmission lines, and 91 load points. An eight-station railway system (Fig. 3(B)) overlaps eight buses in the power system. In addition, four wind farms are assumed to be connected to the power system (at buses 25, 38, 83, and 117) supplying a total power of 60 MW. Two tests,

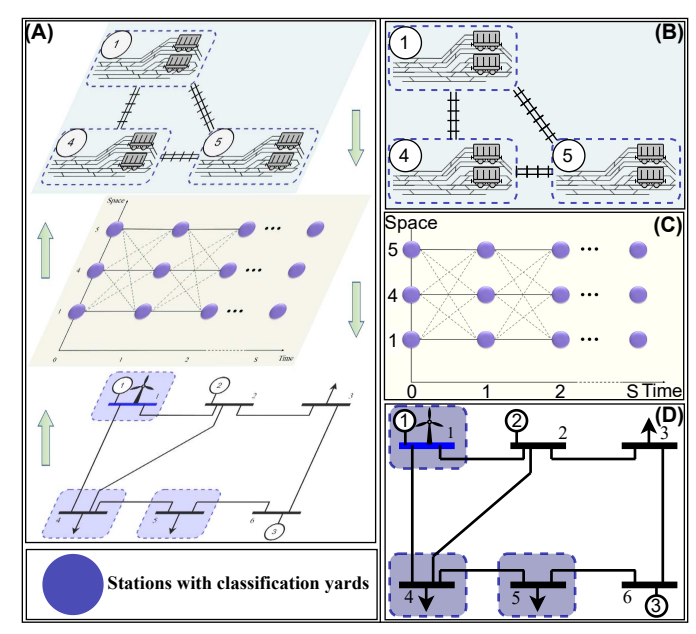


Fig. 1. IEEE 6-bus power system integrated with a railway system. (A) The railway system interacts with a TSN and both networks are linked to the 6-bus power system. (B) There are three railway stations with classification yards that correspond to buses 1, 4, and 5. (C) All stations are connected as represented in the TSN. (D) One-line diagram of the studied power system is illustrated.

one with two BELs and another with three BELs, are carried out and the results are tabulated in Table II. In the two-BEL experiment, each BEL accommodates 200 MWh of energy and ten battery railcars. The three-BEL experiment involves 120 MWh per BEL, totaling six battery railcars.

Results from the first experiment in Table II depict the optimal dispatch of the two BELs in the railway system. In this context, BEL-1 commences its journey at node 117, progressing to node 38. Node 38 functions as an intermediary, granting access to node 77. Once a battery railcar is unloaded at this point, BEL-1 continues its route to node 92, subsequently fulfilling energy needs between the time spans of 4 and 5. Then, it travels back to the starting node and procures the two remaining battery railcars. The second BEL follows a distinct path by initiating from node 25 towards bus 83. It halts at node 83 to deliver the necessary energy before returning to its origin node. The system optimal operation cost amounts to \$1,180,982.215 and allows for 2.43% daily saving as compared to the case where BELs do not move and operate as stationary ESSs. Fig. 2 displays the railway system status at the conclusion of the sixth time span. This illustration clearly showcases the separability characteristic of the battery railcars, emphasizing their distinct performance within the system. The BEL-1 trajectory is in yellow, while the BEL-2's is in green.

In the second experiment, the introduction of a third BEL results in two BELs functioning as stationary ESSs. The optimal BEL dispatch and the number of detached battery railcars are detailed in Table II. The optimal system operation

TABLE II
OPTIMAL BEL DISPATCH IN Case II: IEEE 118-BUS TEST SYSTEM

				First Ex	periment							
	Time span	1	2	3	4	5	6	7	8			
BEL-1	Route (Station <i>i</i> –Station <i>j</i>)	117-38	38-77	77-92	92-92	92-92	92-83	83-25	25-117	Total		
	Required battery railcars	0	1	0	2	3	2	2	0	Operation Cost:		
	Time span	1	2	3	4	5	6	7	8	\$1,180,982.215		
BEL-2	Route (Station <i>i</i> –Station <i>j</i>)	25-83	83-83	83-83	83-83	83-83	83-83	83-83	83-25	\$1,100,902.213		
	Required battery railcars	0	0	3	1	0	1	2	3			
Second Experiment												
	Time span	1	2	3	4	5	6	7	8			
BEL-1	Route (Station <i>i</i> –Station <i>j</i>)	117-117	117-117	117-117	117-117	117-117	117-117	117-117	117-117			
	Required battery railcars	0	0	0	0	0	0	2	4	Total		
	Time span	1	2	3	4	5	6	7	8	Operation Cost:		
BEL-2	Route (Station <i>i</i> –Station <i>j</i>)	25-83	83-92	92-92	92-92	92-92	92-92	92-83	83-25	Operation Cost.		
	Required battery railcars	0	0	2	3	0	1	0	0	\$1,181,607.27		
	Time span	1	2	3	4	5	6	7	8	φ1,101,007.27		
BEL-3	Route (Station <i>i</i> –Station <i>j</i>)	92-92	92-92	92-92	92-92	92-92	92-92	92-92	92-92			
	Required battery railcars	0	0	0	0	0	0	3	3			

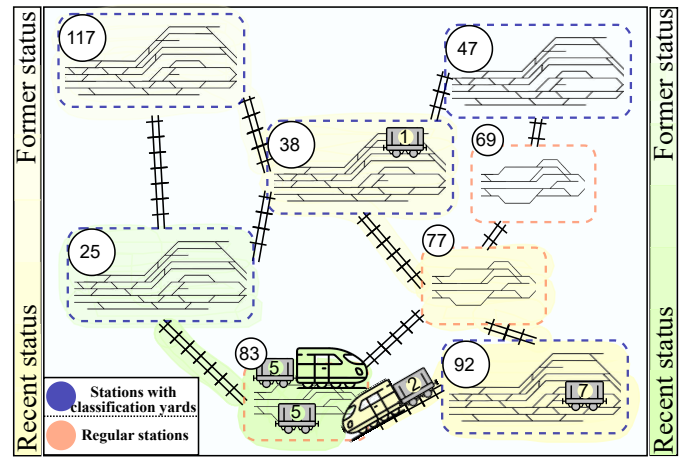


Fig. 2. The status of the railway system and the BELs trajectory (represented by the darkness of the shades) and the number of detached battery railcars (shown on them) at the end of the sixth time span (hour 18). This figure corresponds to the first experiment in *Case II*.

cost for this experiment is determined to be \$1,181,607.27. In this example, a cost saving of 1.35% can be achieved as compared to the stationary BEL configuration. One can thus conclude that BELs may bring about opportunities for cost saving only if strategically deployed and operated.

C. Rationale Behind the Choice of JPC Formulation

In order to assess the superiority of the stochastic programming model with JPCs, a comparative analysis is conducted with a risk-neutral setting wherein the random variables are replaced by their mean values. In order to construct this analysis, 20 new scenarios are generated for the IEEE 6-bus test system at t = 8 (see Table III). The analysis demonstrates the capability of the proposed approach to manage uncertainty and risk in the power system, surpassing the capabilities of the conventional risk-neutral method. Among the generated scenarios, 16 scenarios would lead to an infeasible solution when they are solved with the risk-neutral model. However, none of the scenario realizations would lead to infeasibility when JPCs are employed in the problem formulation. The joint 98% reliability level selected for the JPCs ensures that the system hedges against most adversarial events that could possibly occur. Hence, it can be concluded that the proposed **SMINLP-JPC** formulation accounts for uncertainty while effectively hedging against risk.

D. Computational Efficiency of JPC Reformulations

A performance comparison of the two proposed reformulation methods for the introduced JPCs is provided in Table IV. To assess the computational time required for the reformulation methods, a single BEL is utilized for both the IEEE 6-bus and 118-bus test systems. The energy capacity of the BELs in the 6-bus and 118-bus test systems are considered to be 120 MWh and 200 MWh, respectively. The superiority of the Boolean programming reformulation appears clearly and becomes more pronounced as the number of considered scenarios $|\Omega|$ increases. We consider problem instances with a moderate number (100) of scenarios up to an extremely large number (10,000). Table IV clearly indicates that as the number of scenarios increases, the number of binary variables required to reformulate the problem through scenario-based reformulation rises with the number of scenarios (one binary variable per scenario), resulting in longer computational times. On the other hand, the number of binary variables utilized in the reformulation of the problem using the Boolean method does not vary monotonically with the number of scenarios. This feature enables the model to converge unprecedentedly fast and to achieve an exact solution.

An interesting observation is that, in the Boolean reformulation of the model applied to the IEEE 6-bus test system, the number of constraints and binary variables remains constant regardless of the number of scenarios. However, this is not the case for the scenario-based model which contains a much larger number of constraints and binary variables as the number of scenarios increases. For example, the number of constraints for the 10,000-scenario instance is 77 times greater than the number of constraints for the 100-scenario instance. Similarly, the number of binary variables increases by a factor of approximately 39 when moving from 100 to 10,000 scenarios in the case of the IEEE 6-bus test system. This substantial increase in the number of constraints and binary variables highlights the significant computational costs associated with the scenario-based approach, which becomes

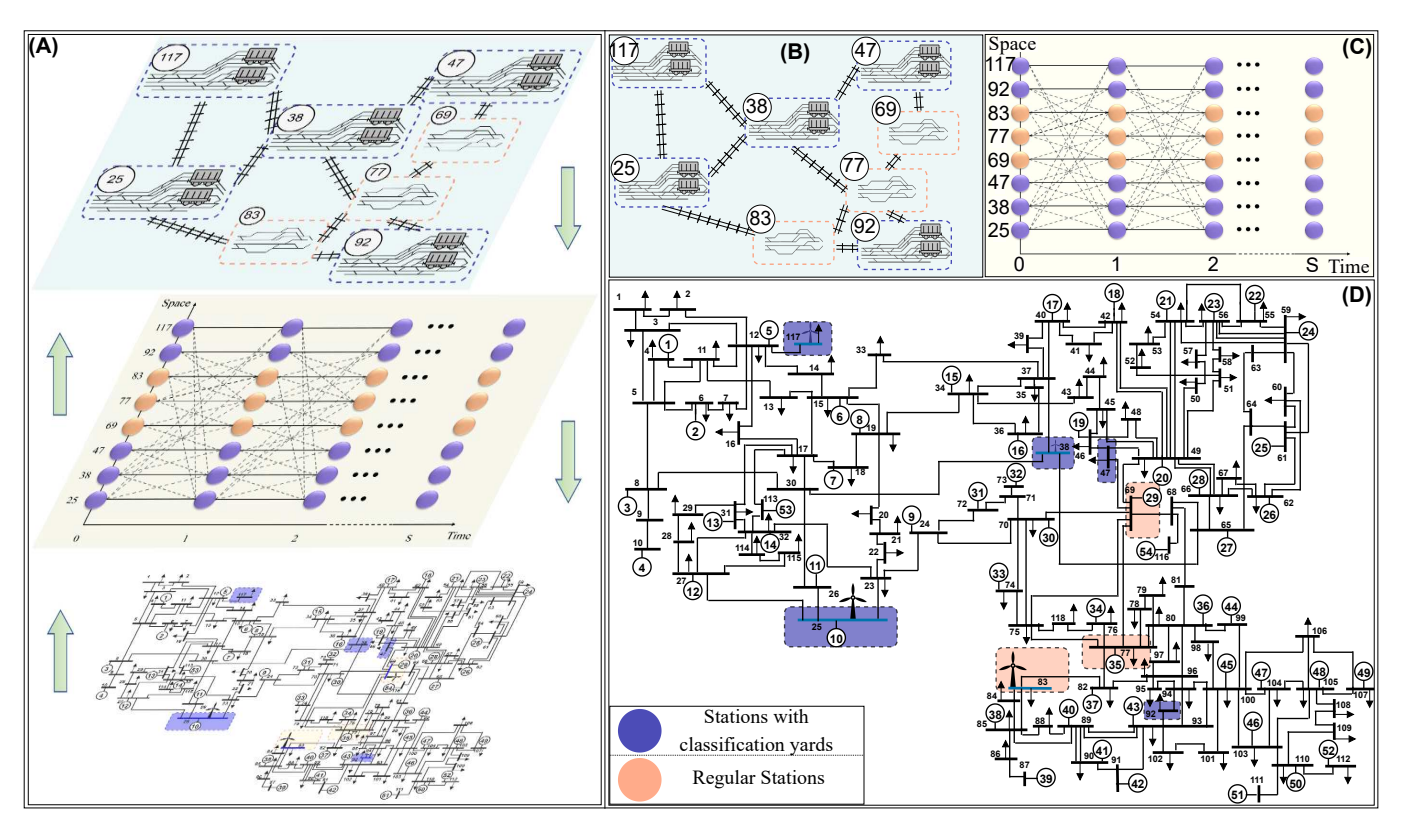


Fig. 3. IEEE 118-bus power systems integrated with a railway system. (A) The 118-bus test system interacts with an eight-station railway system and its associated TSN. (B) The railway system consists of eight railway stations, categorized as the ones with marshalling yards and the regular ones with a capacity of one train. (C) The connections among the railway stations are shown in the TSN. The stations are not all connected and BELs may have to traverse to intermediate stations to get to their final destinations. (D) The one-line diagram of the IEEE 118-bus test system is depicted and the railway stations matching the buses are indicated

untenable for chance-constrained optimization problems with a moderate to large number of scenarios.

For the IEEE 118-bus test system, the Boolean reformulation exhibits a remarkably low increase in the number of constraints when more scenarios are considered. The number of constraints for the 10,000-scenario instance is analogous to the one for the 100-scenario instance, differing only by 17. In a similar vein, the number of binary variables in the Boolean reformulation remains constant for the 100- and 10000-scenario instances. This is in direct contrast to the scenario-based approach that requires the inclusion of 19,800 additional variables when switching from 100 to 10,000 scenarios. Transitioning from 100 to 10,000 scenarios in the IEEE 118-bus test system, the number of constraints in the scenario-based reformulation of the problem grows from 393,441 to 1,739,840. Note also that the number of binary variables

required for the Boolean method in the case of the IEEE 118-bus test problem with 10,000 scenarios is 4,146, which is fewer than the 4,328 binary variables used for the scenario-based reformulation with only 100 scenarios.

Table IV showcases the solution times with the scenario-based approach for up to 1,000 scenarios. The scenario approach cannot solve any of our instances comprising more than 1,000 scenarios in 30 minutes. In contrast, the Boolean reformulation is solved to optimality in less than 10 seconds regardless the considered number of scenarios (up to 10,000). *E. Impacts of BELs on Transmission Line Congestion*

The roles that BEL and transmission lines play in the delivery of power across the network are intertwined. BELs exert a significant influence on reducing the transmission line congestion. In the proposed model, buses with high energy demands that may exceed available transmission capacity are

TABLE III
FEASIBILITY ASSESSMENT OF A RISK-NEUTRAL FORMULATION IN THE PROPOSED MODEL

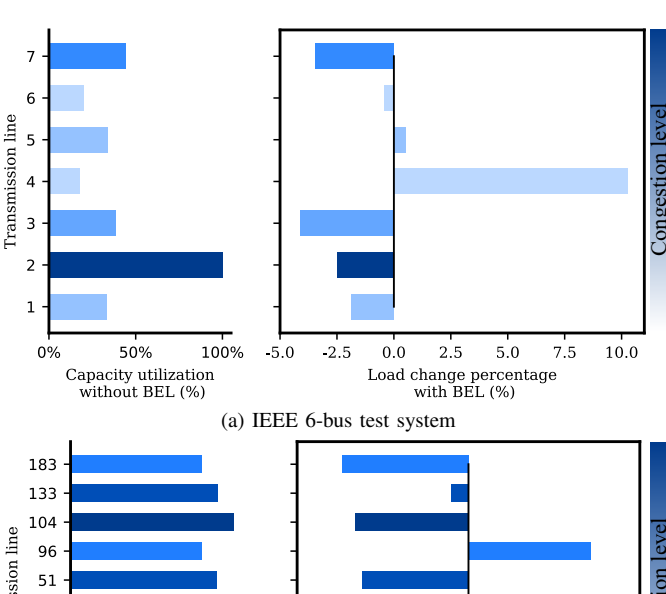
Scenario	$oldsymbol{\xi} = (oldsymbol{\kappa}, \mathbf{p^d}, \mathbf{p^w})$	Feasible?	Scenario	$oldsymbol{\xi} = (oldsymbol{\kappa}, \mathbf{p^d}, \mathbf{p^w})$	Feasible?
1	((3, 1, 3),(71.1, 73, 67.1),(33))	No	11	((2, 3, 2), (68.5, 71.9, 74.1), (26.2))	No
2	((2, 2, 2), (69.5, 66.4, 67), (21.7))	Yes	12	((3, 1, 1), (64.7, 74, 71.4), (17.8))	No
3	((1, 2, 3),(71.6, 64.9, 69.9),(18.2))	No	13	((3, 1, 2), (71.2, 74.6, 71.5), (31.6))	No
4	((3, 3, 3), (67.4, 75.6, 70.5), (28.3))	No	14	((2, 3, 1), (71.1, 67.3, 70.4), (20.8))	No
5	((1, 1, 2),(68.8, 68.1, 62.7),(17))	No	15	((3, 3, 3),(69.9, 69.3, 69.2),(38.5))	Yes
6	((3, 3, 3),(65, 65.1, 66.8),(32.4))	Yes	16	((2, 3, 1), (72.8, 74.2, 71.2), (18.9))	No
7	((3, 2, 2), (70.9, 72.8, 68.9), (24))	No	17	((1, 3, 3), (70.6, 70.4, 76.1), (10.8))	No
8	((2, 1, 2), (66.4, 70.6, 79.6), (32.9))	No	18	((2, 2, 2), (69.8, 68.9, 69.9), (39.4))	Yes
9	((2, 2, 3), (75.9, 70.4, 71.4), (31.4))	No	19	((3, 1, 2), (65.3, 73.2, 70.5), (32.5))	No
10	((2, 1, 2),(71.5, 70.2, 71.3),(29.1))	No	20	((3, 1, 1),(74.4, 73.8, 71.2),(20.7))	No

				Paformula	tion Methods			
Test Systems	$ \Omega $	В	Boolean Programmi		tion iviculous	Objective Value		
		Constraints	Binary Variables	Runtime (s)	Constraints	Binary Variables	Runtime (s)	(\$)
	100	4,196	328	0.1875	16,912	510	26.4688	93,215.94
IEEE 6-Bus	1,000	4,196	328	0.234375	133,012	2,310	N/A (2.45%*)	95,640.15
TEEE 0-Dus	2,000	4,196	328	0.25	262,012	4,310	N/A (4.41%*)	94,543.52
	10,000	4,199	328	0.21875	1,294,010	20,310	N/A (6.83%*)	95,326.75
	100	380,003	4,060	9.54688	393,441	4,242	37.5625	1,183,428.518
IEEE 118-Bus	1,000	380,005	4,060	10.0312	515,841	6,042	N/A (0.01%*)	1,183,566.412
IEEE 110-Dus	2,000	380,005	4,060	9.67188	651,841	8,042	N/A (0.08%*)	1,183,687.016
	10,000	380,020	4,060	9.90625	1,739,840	24,042	N/A (4.61%*)	1,183,812.279

TABLE IV

COMPUTATIONAL PERFORMANCE COMPARISON OF THE REFORMULATION METHODS

identified. These buses are often associated with elevated locational marginal prices, highlighting that there is a monetary incentive to move BELs to supply energy in these locations [14]. To showcase the impacts of BELs on transmission lines, transmission line congestions with and without BELs are compared for the IEEE 6-bus (Case I) and IEEE 118-bus (Case II - second experiment) test systems as displayed in Fig. 4a and Fig. 4b, respectively. In both systems, it is clear that the transmission flow is reduced in highly congested transmission lines. Specifically, in Fig. 4a, the congestion in transmission line 2, connecting bus 1 to bus 4, is mitigated through the BEL traveling to bus 4. The same indications are observed in Fig. 4b where selected transmission lines of the system are analyzed. Evidently, the BELs' integration into the power grid alleviates the burden on highly congested transmission lines by redistributing the flow to lower-loaded lines.



183 - 104 - 104 - 105 -

(b) IEEE 118-bus test system
Fig. 4. Average transmission capacity use without BEL and the congestion relief with BEL. Darker shades reflect higher congestion.

V. DISCUSSIONS

In this section, the practical aspects of the proposed approach are explored, and BEL's applicability with current technological capabilities is evaluated.

A. Investment Cost Recovery of BELs

The existing literature highlights the promising opportunities provided by the integration of BELs with the power system as a mobile grid-support service. Above all, reference [39] draws a comparison between BEL utilization and other feasible investments to enhance power system reliability. The experiments indicate that the utilization of BELs results in savings of \$300 per kW-year compared to the establishment of new transmission lines and a cost reduction of \$85 per kW-year compared to the use of stationary batteries. Study [12] pinpoints the benefits that can be obtained from the optimal utilization of BELs, including demand peak shaving at the national level, increasing power system resiliency in the face of catastrophic events, postponing significant investments to establish new infrastructures, making use of variable renewable energy more efficiently, and reducing power systemdriven emissions. The results of their study indicate a reduction in the system operation costs of up to 3.6%. Note that a modest 2%-3% enhancement in system operation costs can translate into millions of dollars in economic savings within the multi-million dollar electric industry, exceeding the needed investment for BEL integration.

To further justify the utilization of BELs in the day-to-day operation of the power system, a cost-benefit analysis is conducted. This analysis is carried out for the first experiment of *Case II*. The optimal cost attained for this case with the proposed model employing BELs is \$1,180,982.215, whereas, for the case where no BELs are used, the optimal objective value rises to \$1,232,590.223. The result of this study indicates a reduction of approximately 4.34% in the operation costs of the IEEE 118-bus test system when the BELs are employed as a grid support service.

Comparing this value to the capital cost of lithium-ion batteries allows us to conduct the actual cost-benefit analysis. As indicated in [40], [41], it is safe to assume a cost of \$151/kWh for the batteries. Using this cost estimate in our case study, where each BEL carries ten battery-railcars with a capacity of 20MWh, results in a capital cost of \$60,400,000.

^{*}Optimality gap for scenario-based reformulation after 30 minutes

 $TABLE\ V$ Operation Timetable of the Additional Freight Trains in the Railway System

Train-1	Time span	1	2	3	4	5	6	7	8
	Route (Station i -Station j)	38-47	47-69	47-69	69-77	77-92	92-77	77-38	38-38
Train-2	Time span	1	2	3	4	5	6	7	8
	Route (Station <i>i</i> –Station <i>j</i>)	92-92	92-92	92-83	83-25	25-83	83-92	92-92	92-92

TABLE VI
OPTIMAL BEL DISPATCH WITH TRAFFIC CONSIDERATIONS: IEEE 118-BUS TEST SYSTEM

BEL-1	Time span	1	2	3	4	5	6	7	8	Total
	Route (Station i -Station j)	117-38	38-77	77-92	92-92	92-92	92-77	77-38	38-117	Operation Cost:
BEL-2	Time span	1	2	3	4	5	6	7	8	1
	Route (Station <i>i</i> –Station <i>j</i>)	25-83	83-92	92-92	92-92	92-92	92-92	92-83	83-25	\$1,181,086.097

Given that the transportation costs are already accounted for in the mathematical model and a 15-year life-span for the lithium-ion batteries [19], [42], the discounted revenue of the system amounts to \$195,520,788.09 (a 5% yearly interest rate and a 5% yearly battery degradation rate is assumed in our calculations): Discounted revenue = Daily Revenue * 365 (days) * I(P/A,i=5%,n=15).

The comparison between the discounted revenue and the capital cost justifies the application of BELs in monetary terms. This analysis does not necessarily suggest that the utilization of BELs is profitable for every power system regardless of their geographical settings and characteristics, but it showcases the potential of this framework to generate significant cost savings. Moreover, the effect of battery technology advancements on battery price reduction should not be underestimated. As reported in [41], the price of lithiumion batteries experienced around 80% reduction from 2013 to 2022. This cost reduction is expected to continue (and grow) in the future which, in turn, will further enhance the cost-effectiveness of using battery storage solutions such as BELs.

B. Railway Traffic and Itinerary Conflicts

The railway dispatchers have the day-ahead schedule of the other trains [43]. If the schedule of the BELs is to be added to the packed timetable, some readjustments in BELs scheduling are needed. To this aim, we conduct a study to showcase the impact of traffic in the railway system and its ramifications on BELs as well as power system operations. The test is conducted on the first experiment of Case II. The optimal itinerary of BELs without traffic considerations is shown in Table II. Should other trains with distinct routes be considered in the railway system, there will be conflicts between BELs and the other trains. Suppose the eight-station railway system is already scheduled for two trains with the routing and schedule in Table V. Assigning the TSN arcs to the scheduled trains, and fixing their routing in the optimization problem would result in another dispatch schedule for BELs and lead to a slight rise in the optimal system operation costs, as indicated in Table VI. The speed of trains can also be incorporated into the model by adjusting the TSN and adding artificial nodes between the stations.

C. BELs Connection to the Power Grid

In contrast to the typical train classification operations, the BELs and battery railcars are required to undergo a different process that takes much less time. The time it takes to detach the required battery railcars from the BEL is negligible and the BELs can get dispatched to the next stop immediately after the battery railcars are detached. The process of moving the battery railcars through the classification yard and connecting them to the grid may be time-consuming. It is worth mentioning that classification yards and railway stations are already connected to the electrical grid as many switching locomotives (classifier locomotives) operate on electricity. The process of connecting the battery railcar to the grid is also expected to be carried out smoothly without taking considerable time as it does not require blocking processes. In the worst-case scenario, if the classification yard is congested, it can be considered that the connection process for battery railcars could take an entire hourly time period [44] (to account for the length of the connection process, the variable $P'_{k,i,t}$ in JPC (4a) is replaced with $P'_{k,i,t+1}$). The optimal operation costs of the modified power system models still show great potential in terms of cost reduction and economic savings. Table VII indicates the cost-effectiveness of the proposed approach even after consideration of the worst-case latency in connecting the battery railcars to the power grid.

VI. CONCLUSION

In this paper, we develop a new joint probabilistically constrained optimization model for the optimal integration of BELs in power system operation. In line with the national push toward decarbonization and for enhancing renewable energy utilization, BELs play their role as mobile ESSs and absorb the spillage and volatility in renewable energy generation. In the proposed model, the battery railcars attached to the BELs are considered separable which enables a more responsive scheduling of BELs. In addition, the uncertainty in wind generation, load demand, and capacity of the classification yards are explicitly accounted for through the introduction of JPCs. The combination of JPCs and other nonlinear constraints in the proposed SMINLP problem formulation posed severe computational challenges. We have reformulated the SMINLP problem into a tractable deterministic MILP counterpart using a pioneering Boolean programming reformulation method. This reformulation technique allows for the consideration of extremely large numbers of scenarios, thereby providing a more accurate description of uncertainty, while considerably reducing the solution time. The model was applied to and tested on the IEEE 6-bus and IEEE 118-bus test systems to evaluate its efficacy and adaptability. The results showed

TABLE VII

COMPARISON OF THE OPTIMAL SYSTEM OPERATION COSTS IN THE PRESENCE OF THE WORST-CASE LATENCY IN CONNECTING BATTERY RAILCARS

TO THE POWER GRID.

System	# of BELs	# of Scenarios	Optimal Cost		
			Original Model	Modified Model	No BEL Model
IEEE 6-bus Test System	1	10,000	\$95,326.75	\$95,730.9	\$100,553.58
IEEE 118-bus Test System	1	10,000	\$1,183,812.279	\$1,190,417.806	\$1,232,590.223
IEEE 118-bus Test System	2	10,000	\$1,180,982.215	\$1,187,526.551	\$1,232,590.223
IEEE 118-bus Test System	3	10,000	\$1,181,607.27	\$1,188,110.438	\$1,232,590.223

promising cost savings achieved when adopting BELs in power systems proliferated with renewable resources.

Future research could explore the implementation of the proposed framework on the use of BELs for improving the resilience of power grids during extreme events and assess the impact of such technologies on service restoration under challenging operation conditions. In terms of methodology, future research could also explore the ability of AI-based methods to handle nonconvex **SMINLP-JPC** models.

REFERENCES

- A. S. Dagoumas and N. E. Koltsaklis, "Review of models for integrating renewable energy in the generation expansion planning," *Applied Energy*, vol. 242, pp. 1573–1587, 2019.
- [2] A. H. Alobaidi, S. S. Fazlhashemi, M. Khodayar, J. Wang, and M. E. Khodayar, "Distribution service restoration with renewable energy sources: a review," *IEEE Transactions on Sustainable Energy*, 2022.
- [3] M. MansourLakouraj, M. Gautam, H. Livani, M. Benidris, and P. Fajri, "Multi-timescale risk-constrained volt/var control of distribution grids with electric vehicles and solar inverters," in 2021 IEEE PES Innovative Smart Grid Technologies Europe (ISGT Europe), pp. 01–06, IEEE, 2021.
- [4] H. Saboori and S. Jadid, "Mobile and self-powered battery energy storage system in distribution networks—modeling, operation optimization, and comparison with stationary counterpart," *Journal of Energy Storage*, vol. 42, p. 103068, 2021.
- [5] D. Anokhin, P. Dehghanian, M. A. Lejeune, and J. Su, "Mobility-as-a-service for resilience delivery in power distribution systems," *Production and Operations Management*, vol. 30, no. 8, pp. 2492–2521, 2021.
- [6] J. Su, S. Mehrani, P. Dehghanian, and M. A. Lejeune, "Quasi secondorder stochastic dominance model for balancing wildfire risks and power outages due to proactive public safety de-energizations," *IEEE Transactions on Power Systems*, 2023.
- [7] J. Su, D. Anokhin, P. Dehghanian, and M. A. Lejeune, "On the use of mobile power sources in distribution networks under endogenous uncertainty," *IEEE Transactions on Control of Network Systems*, 2023.
- [8] A. Anisie, F. Boshell, S. Kamath, H. Kanani, and S. Mehrotra, "Utility-scale batteries innovation landscape brief," *International Renewable Energy Agency Technical Report*, 2019.
- [9] Massachusetts Department of Energy, "Mobile energy storage study: Emergency response and demand reduction," *Massachusetts Department of Energy Resources*, 2020.
- [10] M. S. AlDavood, A. Mehbodniya, J. L. Webber, M. Ensaf, and M. Azimian, "Robust optimization-based optimal operation of islanded microgrid considering demand response," *Sustainability*, vol. 14, no. 21, p. 14194, 2022.
- [11] H. Hosseinpour, M. MansourLakouraj, M. Ben-Idris, and H. Livani, "Large-signal stability analysis of inverter-based ac microgrids: A critical and analytical review," *IEEE Access*, 2023.
- [12] Y. Sun, Z. Li, M. Shahidehpour, and B. Ai, "Battery-based energy storage transportation for enhancing power system economics and security," *IEEE Transactions on Smart Grid*, vol. 6, no. 5, pp. 2395–2402, 2015.
- [13] Y. Sun, Z. Li, W. Tian, and M. Shahidehpour, "A lagrangian decomposition approach to energy storage transportation scheduling in power systems," *IEEE Trans. Power Syst.*, vol. 31, no. 6, pp. 4348–4356, 2016.
- [14] Y. Sun, J. Zhong, Z. Li, W. Tian, and M. Shahidehpour, "Stochastic scheduling of battery-based energy storage transportation system with the penetration of wind power," *IEEE Transactions on Sustainable Energy*, vol. 8, no. 1, pp. 135–144, 2016.
- [15] R. Ebadi, A. S. Yazdankhah, B. Mohammadi-Ivatloo, and R. Kazemzadeh, "Coordinated power and train transportation system with transportable battery-based energy storage and demand response: A multi-objective stochastic approach," *Journal of Cleaner Production*, vol. 275, p. 123923, 2020.

- [16] R. Ebadi, A. S. Yazdankhah, R. Kazemzadeh, and B. Mohammadi-Ivatloo, "Techno-economic evaluation of transportable battery energy storage in robust day-ahead scheduling of integrated power and railway transportation networks," *International Journal of Electrical Power & Energy Systems*, vol. 126, p. 106606, 2021.
- [17] M. A. Mirzaei, M. Hemmati, K. Zare, B. Mohammadi-Ivatloo, M. Abapour, M. Marzband, and A. Farzamnia, "Two-stage robuststochastic electricity market clearing considering mobile energy storage in rail transportation," *IEEE Access*, vol. 8, pp. 121780–121794, 2020.
- [18] M. A. Mirzaei, M. Hemmati, K. Zare, B. Mohammadi-Ivatloo, M. Abapour, M. Marzband, R. Razzaghi, and A. Anvari-Moghaddam, "Network-constrained rail transportation and power system scheduling with mobile battery energy storage under a multi-objective two-stage stochastic programming," *International Journal of Energy Research*, vol. 45, no. 13, pp. 18827–18845, 2021.
- [19] G. Pulazza, N. Zhang, C. Kang, and C. A. Nucci, "Transmission planning with battery-based energy storage transportation for power systems with high penetration of renewable energy," *IEEE Transactions* on *Power Systems*, vol. 36, no. 6, pp. 4928–4940, 2021.
- [20] J. Yan, F. Lai, Y. Liu, C. Y. David, W. Yi, and J. Yan, "Multi-stage transport and logistic optimization for the mobilized and distributed battery," *Energy Conversion and Manage.*, vol. 196, pp. 261–276, 2019.
- [21] Y. Yan, W.-L. Shang, J. Yan, Q. Liao, B. Wang, H. Song, and Y. Liu, "Logistic and scheduling optimization of the mobilized and distributed battery in urban energy systems," *Resources, Conservation and Recy*cling, vol. 187, p. 106608, 2022.
- [22] L. Meng and X. Zhou, "Robust single-track train dispatching model under a dynamic and stochastic environment: A scenario-based rolling horizon solution approach," *Transportation Research Part B: Method-ological*, vol. 45, no. 7, pp. 1080–1102, 2011.
- [23] A. D'Ariano, L. Meng, G. Centulio, and F. Corman, "Integrated stochastic optimization approaches for tactical scheduling of trains and railway infrastructure maintenance," *Computers & Industrial Engineering*, vol. 127, pp. 1315–1335, 2019.
- [24] A. A. Khaled, M. Jin, D. B. Clarke, and M. A. Hoque, "Train design and routing optimization for evaluating criticality of freight railroad infrastructures," *Transport. Res. P. B: Method.*, vol. 71, pp. 71–84, 2015.
- [25] T. Lidén and M. Joborn, "An optimization model for integrated planning of railway traffic and network maintenance," *Transportation Research Part C: Emerging Technologies*, vol. 74, pp. 327–347, 2017.
- [26] C. Zhang, Y. Gao, L. Yang, Z. Gao, and J. Qi, "Joint optimization of train scheduling and maintenance planning in a railway network: A heuristic algorithm using lagrangian relaxation," *Transportation Research Part B: Methodological*, vol. 134, pp. 64–92, 2020.
- [27] H. Zhang, S. Li, Y. Wang, L. Yang, and Z. Gao, "Collaborative real-time optimization strategy for train rescheduling and track emergency maintenance of high-speed railway: A lagrangian relaxation-based decomposition algorithm," *Omega*, vol. 102, p. 102371, 2021.
- [28] X. Geng and L. Xie, "Data-driven decision making in power systems with probabilistic guarantees: Theory and applications of chance-constrained optimization," Ann. Rev. in Con., vol. 47, pp. 341–363, 2019.
- [29] G. P. McCormick, "Computability of global solutions to factorable nonconvex programs: Part I—convex underestimating problems," *Mathematical Programming*, vol. 10, no. 1, pp. 147–175, 1976.
- [30] M. Asghari, A. M. Fathollahi-Fard, S. Mirzapour Al-e hashem, and M. A. Dulebenets, "Transformation and linearization techniques in optimization: A state-of-the-art survey," *Mathematics*, vol. 10, no. 2, p. 283, 2022.
- [31] M. A. Lejeune, "Pattern-based modeling and solution of probabilistically constrained optimization problems," *Operations Research*, vol. 60, no. 6, pp. 1356–1372, 2012.
- [32] A. Kogan and M. A. Lejeune, "Threshold boolean form for joint probabilistic constraints with random technology matrix," *Mathematical Programming*, vol. 147, pp. 391–427, 2014.

- [33] M. A. Lejeune and F. Margot, "Solving chance-constrained optimization problems with stochastic quadratic inequalities," *Operations Research*, vol. 64, no. 4, pp. 939–957, 2016.
- [34] F. Kochakkashani, P. Dehghanian, and M. A. Lejeune, "On the use of battery-electric locomotive as a grid-support service in electric power systems," 2024. Electronic Appendix. [Online]. Available: https://blogs.gwu.edu/seas-payman-lab/files/2024/01/ Appendix-ca1c48fe855aefec.pdf.
- [35] N. Boaretto, I. Garbayo, S. Valiyaveettil-SobhanRaj, A. Quintela, C. Li, M. Casas-Cabanas, and F. Aguesse, "Lithium solid-state batteries: State-of-the-art and challenges for materials, interfaces and processing," *Journal of Power Sources*, vol. 502, p. 229919, 2021.
- [36] U. o. W. Clean Energy Institute, "Lithium-ion battery." [Online]. Available: https://www.cei.washington.edu/research/energy-storage/lithium-ion-battery, 2023.
- [37] CSX, "Railroad equipment." [Online]. Available: https://www.csx.com/index.cfm/customers/resources/equipment/railroad-equipment, 2023.
- [38] F. Corman, A. D'Ariano, D. Pacciarelli, and M. Pranzo, "Optimal inter-area coordination of train rescheduling decisions," *Transportation Research Part E: Logistics and Transportation Review*, vol. 48, no. 1, pp. 71–88, 2012.
- [39] J. W. Moraski, N. D. Popovich, and A. A. Phadke, "Leveraging rail-based mobile energy storage to increase grid reliability in the face of climate uncertainty," *Nature Energy*, pp. 1–11, 2023.
- [40] NREL, "Utility-scale battery storage." [Online]. Available: https://atb.nrel.gov/electricity/2021/utility-scale_battery_storage, 2023.
- [41] Bloomberg, "Lithium-ion battery pack prices rise for first time to an average of \$151/kwh." [Online]. Available: https://about.bnef.com/blog/ lithium-ion-battery-pack-prices-rise-for-first-time-to-an-average-of-151-kwh, 2022
- [42] X. Hu, L. Xu, X. Lin, and M. Pecht, "Battery lifetime prognostics," *Joule*, vol. 4, no. 2, pp. 310–346, 2020.
- [43] F. F. Pashchenko, N. A. Kuznetsov, N. Ryabykh, I. Minashina, E. Zakharova, and O. Tsvetkova, "Implementation of train scheduling system in rail transport using assignment problem solution," *Procedia Computer Science*, vol. 63, pp. 154–158, 2015.
- [44] N. Minbashi, C.-W. Palmqvist, M. Bohlin, and B. Kordnejad, "Statistical analysis of departure deviations from shunting yards: Case study from swedish railways," *Journal of Rail Transport Planning & Management*, vol. 18, p. 100248, 2021.



Miguel Lejeune is a Professor at the Department of Decision Sciences and has a courtesy appointment at the Department of Electrical and Computer Engineering at the George Washington University (GWU). Prior to joining GWU, he was a Visiting Assistant Professor in Operations Research at Carnegie Mellon University. He held visiting positions at Carnegie Mellon University, Georgetown University, the University of California – Irvine, and the Foundation Getulio Vargas in Rio de Janeiro. He is the recipient of the 2019 Koopman Award of the

INFORMS Society, a CAREER/Young Investigator Research Grant from the Army Research Office, and the IBM Smarter Planet Faculty Innovation Award. Dr. Lejeune's areas of expertise include stochastic programming, distributionally robust optimization, and data-driven optimization with applications in finance, supply chain management, health care, and energy. His current research is funded by the National Science Foundation, the Office of Naval Research, and the DUKE Energy Innovation Fund.



Farid Kochakkashani (Graduate Student Member, IEEE) received the M.Sc. degree in industrial engineering from Sharif University of Technology, Tehran, Iran, in 2022. He is currently pursuing the Ph.D. degree in electrical engineering with the Department of Electrical and Computer Engineering, George Washington University, Washington, D.C., USA. His research interests include mathematical optimization and its applications in power system planning and operation, power system reliability and resiliency, and energy economics.



Payman Dehghanian (Senior Member, IEEE) is currently an Associate Professor with the Department of Electrical and Computer Engineering at the George Washington University, Washington, D.C., USA. He received the B.Sc., M.Sc., and Ph.D. degrees all in Electrical Engineering respectively from University of Tehran, Tehran, Iran, in 2009, Sharif University of Technology, Tehran, Iran, in 2011, and Texas A&M University, Texas, USA in 2017. His research interests include power system reliability and resilience assessment, data-informed decision-

making for maintenance and asset management in electrical systems, and smart electricity grid applications.

Dr. Dehghanian is the recipient of the 2014 and 2015 IEEE Region 5 Outstanding Professional Achievement Awards, the 2015 IEEE-HKN Outstanding Young Professional Award, the 2021 Early Career Award from the Washington Academy of Sciences, and the 2022 Early Career Researcher Award from the George Washington University.